Line Shapes, Saturation Behavior, and Temperature Studies in the Nuclear Resonance of Nickel

R. L. STREEVER AND L. H. BENNETT
National Bureau of Standards, Washington, D. C.
(Received 10 December 1962; revised manuscript received 21 May 1963)

The nuclear magnetic resonance of Ni^{61} has been studied in pure nickel powders. Both natural nickel (1.25% abundant in Ni^{61}) and enriched nickel (99.9% abundant in Ni^{61}) were used. The signal observed with a circuit sensitive to the absorption of power is a combination of absorption and dispersion modes. The amount of mode mixing is found to depend on the applied rf field, ambient temperature, annealing temperature, and external magnetic-field intensity. The mode mixing of the resonance is related to electronic losses in the sample. The saturation behavior of the individual absorption and dispersion modes is that of an inhomogeneously broadened line. From the saturation behavior an estimate of the enhancement of the applied rf level for nuclei in domain walls of about 7×10^3 is made. An additional broadening mechanism is observed in the enriched nickel, particularly at 77°K. Application of Redfield's theory of saturation at high rf levels leads to the conclusion that the additional broadening can be attributed to strong indirect exchange between nuclei. Frequency measurements from room temperature to 4.2°K made with a marginal oscillator in both the enriched and unenriched nickel are presented. A temperature-dependent frequency shift is found between the enriched and unenriched nickel which appears to be a maximum at about 200°K where the enriched nickel frequency is about 30 kc/sec higher. From room temperature to 536°K, frequency measurements made with super-regenerative circuits are reported. A comparison of the temperature dependence of the resonance frequency with the saturation magnetization is made.

I. INTRODUCTION

NUCLEAR magnetic resonance in ferromagnetic materials, such as nickel metal, differs from that in nonferromagnetic materials in several respects. Gossard and Portis[1,2] have shown that, in multidomain ferromagnetic materials, the nuclei are not driven directly by the applied rf field, but first the applied field causes motion of the domains and domain walls. This motion, in turn, through the hyperfine interaction between the electronic magnetization and nuclear magnetization, causes an rf field at the nuclei at right angles to the hyperfine field. This effective rf field at the nucleus is greatly enhanced over the applied rf field. Furthermore, as a result of magnetic losses in the sample, the nuclei are excited by components of the electronic magnetization both in and out of phase with respect to the applied rf field, resulting in a mixture of absorption and dispersion modes[3] in the observed nuclear signal. Finally, in these materials, the resonance lines are generally inhomogeneously broadened, and the saturation behavior is that of an inhomogeneously broadened[4] line.

In this work we have studied the nuclear resonance of Ni^{61} in pure nickel metal.[5] Using a circuit sensitive only to the power absorbed, the nuclear resonance signal observed is found to be a combination of absorption and dispersion modes. The relative amounts of absorption and dispersion present has been studied as a function of applied rf field, state of anneal of the samples, external dc magnetic field, and temperature. Experimental techniques are presented in Sec. II. A theory of the line shape and the saturation behavior of the individual absorption and dispersion modes is given in Sec. III. A discussion of the application of Portis' theory of inhomogeneous broadening[4] and Redfield's theory of saturation[6] at high rf levels to nuclear resonance in nickel is given. The experimental observations at room temperature are presented in Secs. IV (A) and IV (B). These studies of line shape and saturation behavior are interesting in themselves since they yield information about the enhancement of the rf field at the nuclei, the damping of the electronic motion, and, in the case of the enriched nickel, about the interactions between the nuclei. They are also important since accurate measurements of linewidth and frequency also depend on an understanding of the line shape. In Sec. IV (C) we present the temperature dependence of the Ni^{61}, resonance frequency, and width obtained in a consistent way based on the studies of the line shape.

II. EXPERIMENTAL TECHNIQUES

A. Samples

The nuclear resonance of Ni^{61} was studied in both natural nickel (1.25% abundant in Ni^{61}) and in enriched nickel (99.9% abundant in Ni^{61}). For the same quantity of sample (2 g), the enriched nickel showed a resonance at room temperature about twenty times as large, in amplitude, as the best sample of unenriched nickel. The additional factor of 5 improvement, which might have been expected, was not found due to the larger linewidth and poorer annealing of the enriched nickel. This larger width is attributed to impurities (mainly about 0.1% aluminum), residual strain, and effects of

[1] A. C. Gossard, Ph.D. thesis, University of California, 1960 (unpublished).
[2] A. C. Gossard and A. M. Portis, Suppl. J. Appl. Phys. **31**, 205, (1960).
[3] W. A. Hardy, Suppl. J. Appl. Phys. **32**, 122 (1961).
[4] A. M. Portis, Phys. Rev. **91**, 1071 (1953).
[5] L. H. Bruner, J. I. Budnick, and R. J. Blume, Phys. Rev. **121**, 83 (1961).
[6] A. G. Redfield, Phys. Rev. **98**, 1787 (1955).

the rf field. For room temperature measurements, a 10-g sample of the best unenriched nickel made up for some of the advantages of the enrichment.

The unenriched nickel was 99.999% pure, with an average particle size less than 10 μ. Less pure nickel gave substantially the same results, but poorer signal to noise, owing to the increased linewidth. The most intense signals were found for a sample annealed for one hour at 1100°C. The annealing was carried out in a nickel boat under hydrogen. The hydrogen was pumped out after the temperature was lowered by about 200°C. Sintering of the fine particles was avoided by mixing the nickel powder with high purity Al_2O_3 powder. The Al_2O_3 was separated magnetically after annealing.

The effects of strain were studied on nickel powder produced by an atomization method which put strains in it, and on powder produced by filing. No resonance was observable in the extremely cold worked (as filed) sample.

B. Equipment

Almost all the measurements reported here were made using a marginal push-pull oscillator[7] which operates with good sensitivity over a range of rf levels between about 300 mV and 1.5 V. The spectrometer was frequency modulated at 40 cps. The first derivative of the resonance line was observed by the usual technique of small sine-wave modulation, along with a conventional lock-in amplifier and detector system operating at the fundamental modulation frequency. The second derivative was observed with the same equipment, but the fundamental modulation frequency was rejected, the second harmonic being amplified and detected. The latter method had the advantage, especially for broader lines, of reducing the large modulation leakage which arises from spurious amplitude modulation. In either case, it was essential to avoid overmodulation which distorts and shifts the resonance line. The effect of overmodulation on the line shape resembles the mode mixing discussed in this paper and makes comparisons of lines measured under different conditions difficult. The best signal to noise was obtained, of course, for a modulation amplitude which was too high for line shape studies.

One peculiarity about nuclear resonance in ferromagnetic materials is that the sample itself is a large perturbation on the operation of the spectrometer. Hence, when comparisons are made between different samples, care must be taken to use samples which are as similar, macroscopically, as possible. Also, since the presence of a magnetic sample severely reduces the Q of the coil, there is not as great an advantage in filling the coil completely as there is for less lossy samples.

The low-temperature measurements were made using a Dewar, the finger of which fits into the rf coil. The sample is capsulated in glass and held stationary with frozen paraffin oil.[8] For the liquid-helium runs, the helium reservoir was surrounded by liquid nitrogen, but no nitrogen was used to surround the finger in the coil. The largest heat source was in the finger. The Dewar used about 4 liters of helium which lasted several hours.

Some of the measurements, particularly the frequency at temperatures above room temperature, were made using a super-regenerative oscillator. This had the advantage of presenting a strong signal on the oscilloscope, which permitted following visually the change of resonance frequency with temperature; hence, it was less likely to mistake a spurious signal for a resonance. Of course, the super-regenerative circuit is not suitable for line shape determinations.

III. THEORY OF THE LINE SHAPE AND SATURATION

Gossard, in his thesis[1] on nuclear resonance in ferromagnetic materials, has derived an expression for the signal observed using a circuit sensitive to the rf power absorbed by a ferromagnetic sample. He shows that the observed power loss is due to a modulation of electronic losses by the nuclear precession. The part of the power absorbed which is due to the nuclei is a combination of χ', the real part of the complex nuclear susceptibility, and χ'', the imaginary part. There is thus, built into the ferromagnetic sample, a mechanism which mixes modes.

The applied rf field causes domain wall motion and also domain rotation which, through the hyperfine interaction between the electrons and the nuclei, gives rise to a field at the nuclei, perpendicular to their polarization direction. The effective rf field at the nucleus is much larger than the applied rf field, and this enhancement is responsible for the large signals observed. Domain wall excitation is believed to give rise to a larger enhancement than domain rotation. Assuming the Landau-Lifshitz equations for the motion of the electrons, Gossard[9] has derived an equation for the power absorbed by the sample for the case of domain wall excitation,

$$\frac{dW}{dt}=\lambda H_{d0}^2\left[1+\frac{\gamma_e H_N^2\chi'}{M\omega}+\frac{\gamma_e^2 H_N^2\chi''}{\lambda\omega}\right], \qquad (1)$$

where H_N=nuclear hyperfine field, M=saturation magnetization, γ_e=electron gyromagnetic ratio, and λ=electronic damping coefficient in the Landau-Lifshitz equation:

$$d\mathbf{M}/dt=\gamma(\mathbf{M}\times\mathbf{H})-(\lambda/M^2)(\mathbf{M}\times\mathbf{M}\times\mathbf{H}).$$

H_{d0}=demagnetization field in plane perpendicular to wall in absence of nuclei. The first term in Eq. (1) represents wall losses, and is independent of frequency

[7] Similar to that described in G. Benedek and Y. Kushida, Phys. Rev. **118**, 46 (1960); and R. G. Shulman, *ibid.* **121**, 125 (1961).

[8] R. J. Snodgrass and L. H. Bennett, Appl. Spectry. **17**, 53 (1963).

[9] Ref. 1, p. 51.

for rf frequencies. The last two terms are the nuclear losses which can be rewritten as

$$\frac{dW}{dt}=\frac{H_{d0}^2\gamma_e H_N^2\lambda}{M\omega\beta_0}(\chi''+\beta_0\chi'), \tag{2}$$

where $\beta_0=\lambda/M\gamma_e$. An effective value H_2 of the driving field at the nucleus can be defined by rewriting Eq. (2)

$$dW/dt=2H_2^2\omega\chi_2'', \tag{3}$$

where

$$\chi_2''=\chi''+\beta_0\chi', \quad \text{and} \quad H_2=H_{d0}\gamma_e/\sqrt{2}\gamma_n. \tag{4}$$

χ_2'' is the effective value of the imaginary part of the nuclear susceptibility. γ_n is the gyromagnetic ratio of the nucleus. The constant β_0 which determines the amount of mode mixing will depend on the electronic losses of the sample, since β_0 is proportional to the electronic damping coefficient which enters into the Landau-Lifshitz equations. The greater the damping of the electronic magnetization the greater will be the mode mixing.

The parameter β_0 is expected to vary from material to material. Smit and Wijn[10] gave a typical value of β_0 of 0.01, which is presumably for a ferrite. For a metal with large eddy current losses, the major contribution to β_0 might be expected to arise from eddy current damping of the domain wall motion. Winter[11] shows that the nuclear spin-lattice relaxation time in a ferromagnetic metal will depend on the value of β_0, and he finds that a value of β_0 of about 0.02 is needed to give the observed value of T_1 in nickel.

In nuclear resonance in nonferromagnetic metals in which the nuclei are driven directly by the applied rf field, mode mixing is observed in thick samples due to the fact that the rf field inside the metal gets out of phase with that at the surface of the metal[12,13] as a result of eddy currents. The amount of mode mixing is found to depend on the ratio of particle diameter d to the skin depth δ. For a spherical particle with $d/\delta\gg1$ the value of β_0 is about 0.7. One can calculate the skin depth in the nickel particles used. With a magnetic permeability $\mu=200$, a resistivity $\rho=6.8\times10^{-6}$ Ω-cm and a frequency of 27 Mc/sec, the skin depth $\delta=1.6\times10^{-4}$ cm. The particle diameter d is 10^{-3} cm, then $d/\delta=6$. This value of μ holds for a well-annealed sample.[14] For a poorly annealed sample, μ is or the order of 100 or less,[14] so d/δ is about four. At low rf level we expect that if this mechanism would apply there would be an approximately equal mixture of absorption and dispersion.

In the case of a ferromagnetic metal, however, where the major nuclear signal arises from domain wall motion, the mode mixing caused by the above mechanism is expected to be smaller, since if we assume Eq. (1) is valid even in the presence of eddy currents, we see that only the phase shift between H_{d0} and the nuclei is important. Thus, while the effect of eddy currents will increase the damping of the domain wall motion and in this way increase the mode mixing, the effect of dephasing between the rf field outside the metal and that inside the metal as a direct result of skin depth is probably much less important in the case of domain wall excitation than it is for nuclear resonance, in which the nuclei are driven directly by the rf field. Hence, a β_0 of about 0.02 is more appropriate for domain wall excitation.

The signal observed in the absence of saturation effects, using an absorption type circuit, will then be proportional to $H_2(\chi''+\beta_0\chi')$, $H_2\beta_0\chi'$ being the observed dispersion signal and $H_2\chi''$ being the observed absorption signal. Since χ' and χ'' themselves depend on H_2, we must consider how these nuclear susceptibilities behave for an inhomogeneously broadened line. For an inhomogeneously broadened line Portis[4,15] finds

$$\chi''=\frac{\chi_0\omega_0T_2^*}{2}\left[\frac{1}{1+T_2^{*2}(\omega-\omega_0)^2}\right](1+\gamma^2H_2^2T_1T_2)^{-1/2}, \tag{5}$$

$$\chi'=\frac{\chi_0\omega_0T_2^*}{2}\left[\frac{(\omega-\omega_0)T_2^*}{1+T_2^{*2}(\omega-\omega_0)^2}\right], \tag{6}$$

where T_1 = longitudinal relaxation time, T_2 = transverse relaxation time, and T_2^* = parameter determining width of inhomogeneously broadened line.

In deriving Eqs. (5) and (6), Lorentz shapes were assumed for individual spin packets as well as for their envelopes. The above equations also assume that the inhomogeneous linewidth, $\Delta H=2/\gamma T_2^*$, is such that $T_2^*\ll T_2$. This is nearly valid for pure unenriched nickel where[16] $T_2=0.35$ msec and $T_2^*=0.01$ msec. It is also assumed that H_2, the effective rf field, is much less than the inhomogeneous linewidth ΔH, in gauss. Under these conditions we see that χ'' does not change shape on saturation, but decreases in magnitude with a factor $(1+\gamma^2H_2^2T_1T_2)^{-1/2}$. χ' remains undiminished with increasing H_2 and has a shape derived from the unsaturated absorption through the Kronig-Kramers relations. When H_2 becomes comparable to the linewidth in gauss, the above rules break down and χ' saturates. The absorption and dispersion lines broaden to a value $\Delta H'=2/\gamma T_2^{*\prime}$ where

$$\frac{1}{T_2^{*\prime}}=\frac{1}{T_2^*}+\frac{1}{T_2}(1+\gamma^2H_2^2T_1T_2)^{1/2}. \tag{7}$$

The line shapes observed in nuclear magnetic reso-

[10] J. Smit and H. P. J. Wijn, *Ferrites* (John Wiley & Sons, Inc., New York, 1959), p. 102.
[11] J. M. Winter, Phys. Rev. **124**, 452 (1961).
[12] N. Bloembergen, J. Appl. Phys. **23**, 1383 (1952).
[13] A. C. Chapman, P. Rhodes, and E. F. W. Seymour, Proc. Phys. Soc. (London) **70**, 345 (1957).
[14] R. M. Bozorth, *Ferromagnetism* (D. Van Nostrand, Inc., Princeton, New Jersey, 1952), pp. 274–275.
[15] A. Abragam, *The Principles of Nuclear Magnetism* (Oxford University Press, New York, 1961).
[16] M. Weger, E. L. Hahn and A. M. Portis, Suppl. J. Appl. Phys. **32**, 124 (1961).

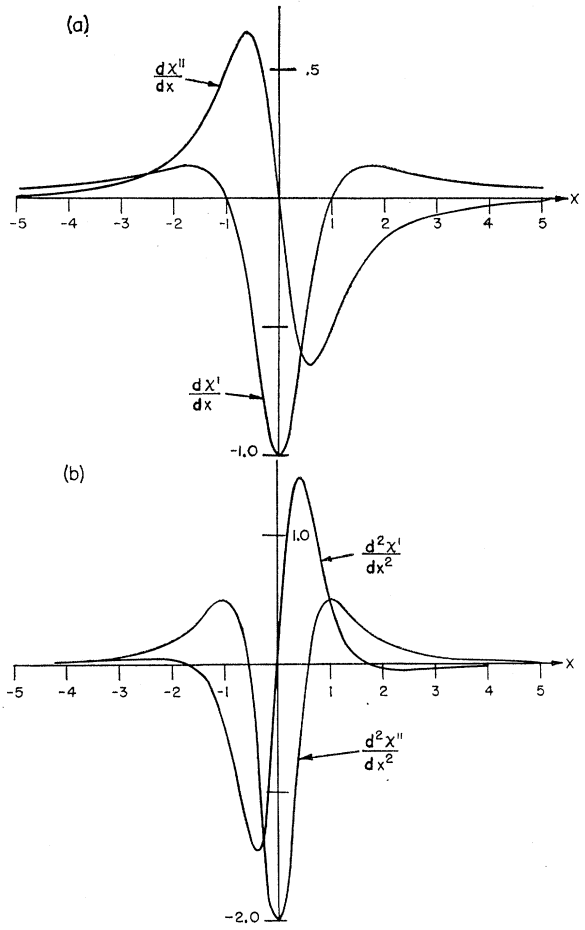

FIG. 1. (a) First derivative of nuclear susceptibilities χ' and χ'' plotted against the parameter $x=\omega_0 T_{2e}$. (b) Second derivatives of the susceptibilities.

nance can be derived by solving the Bloch equations for the nuclear magnetization. These equations lead to the following relations for the real and imaginary parts of the complex nuclear susceptibility, $\chi=\chi'+i\chi''$, if the rf level is low enough so that saturation effects are absent:

$$\chi''=\frac{\chi_0\omega_0 T_2}{2}\frac{1}{1+T_2^2(\omega-\omega_0)^2}, \tag{8}$$

$$\chi'=\frac{\chi_0\omega_0 T_2}{2}\frac{T_2(\omega-\omega_0)}{1+T_2^2(\omega-\omega_0)^2}. \tag{9}$$

Equations (5) and (6) reduce to Eqs. (8) and (9) if $H_2=0$ and $T_2=T_2^*$.

These line shapes have the Lorentz form, and are consistent with the Kronig-Kramers relations. In Fig. 1(a) we plot the first derivatives[17] of the susceptibilities χ'' and χ', while in Fig. 1(b) we plot the second derivatives of the susceptibilities against the parameter $x=(\omega-\omega_0)T_2$.

Gaussian line shapes can be easily distinguished from the Lorentz shape by noting the ratios of suitable peaks of the theoretical resonance curves. Table I shows the ratio of the larger maximum (or maxima) to the smaller maximum (or maxima) for the Gaussian and the Lorentz shape for first and second derivatives of the absorption and dispersion.

TABLE I. The ratio of the larger peak to the smaller peak for first and second derivatives of the Lorentz and Gaussian shapes.

	1st derivative		2nd derivative	
	Absorption	Dispersion	Absorption	Dispersion
Lorentz	1:1	8:1	4:1	40:1
Gauss	1:1	3.5:1	2.2:1	6.7:1

Quite generally, when there is a mixture of absorption and dispersion modes with the same width, the experimentally observed resonance signal S can be written (assuming a Lorentz shape):

$$S(x)=A\left(\frac{1}{1+x^2}+\beta\frac{x}{1+x^2}\right), \tag{10}$$

where $x=T_{2e}(\omega-\omega_0)$. T_{2e} is associated with the experimental width. We will express our measured linewidth by $\Delta\nu=1/\pi T_{2e}$ in this paper. The parameter β determines the amount of absorption and dispersion present and A the amplitude of the signal. A is the peak absorption signal, while βA is the peak-to-peak dispersion signal. The ratio of peak absorption signal to peak-to-peak dispersion signal is just β. If a Lorentz line shape is assumed, a theoretical curve of the ratio of the two larger peaks of the theoretical resonance curve can be plotted (see insert, Fig. 2) as a function of β. This curve

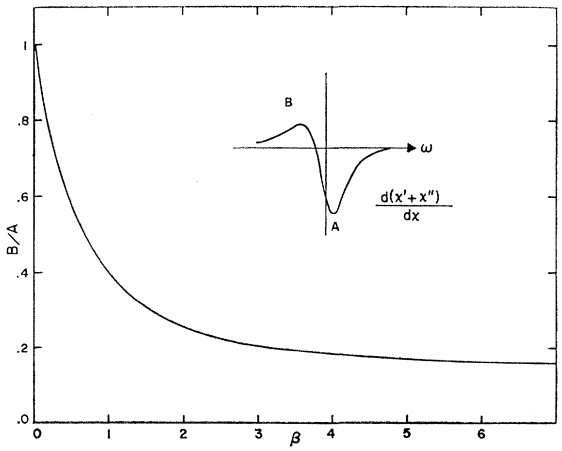

FIG. 2. A plot of the ratio of the smaller peak B to the larger peak A of the theoretical resonance curve plotted against the mode mixing parameter β. Shown in the insert is plot of the first derivative of the resonance curve for the case of $\beta=1$.

[17] For a discussion of line shapes in nuclear magnetic resonance see G. E. Pake and E. M. Purcell, Phys. Rev. 74, 1184 (1948).

is shown in Fig. 2 and can be used to determine β from the experimental resonance curves.

From Eq. (4) the observed signal is

$$S(\omega)=\chi_2''H_2=H_2(\chi''+\beta_0\chi'). \tag{11}$$

When the inhomogeneous broadening theory is applicable, we have, substituting Eq. (5) and (6) in (11),

$$S(\omega)=\frac{H_2\chi_0\omega_0T_2^*}{2}\times\left\{\left[\frac{1}{1+T_2^{*2}(\omega-\omega_0)^2}\right](1+\gamma^2H_2^2T_1T_2)^{-1/2}+\beta_0\left[\frac{(\omega-\omega_0)T_2^*}{1+T_2^{*2}(\omega-\omega_0)^2}\right]\right\}. \tag{12}$$

Finally, by relating Eqs. (10) and (12), we have

$$A=\tfrac{1}{2}\chi_0\omega_0T_2^*H_2(1+\gamma^2H_2^2T_1T_2)^{-1/2}, \tag{13}$$

$$\beta=\beta_0(1+\gamma^2H_2^2T_1T_2)^{1/2}. \tag{14}$$

$\Delta\nu=1/\pi T_{2e}$ is width at half-maximum of the absorption curve. (15)

We have thus far in the analysis neglected the way Redfield's result[6] modifies the above analysis. In the case $T_1=T_2$, one expects the Bloch equations to be valid. In unenriched nickel this condition is approximately fulfilled.[16]

When $\gamma^2H_2^2T_1T_2\gg1$, Eq. (7) gives

$$1/T_2^{*\prime}=(1/T_2^*)+\gamma H_2(T_1/T_2)^{1/2},$$

which does not correctly describe the line broadening with high rf levels when $T_1\neq T_2$.

At large rf levels, well beyond the region where the absorption saturates out, $(\gamma^2H_2^2T_1T_2\gg1)$, Redfield[6] showed that χ' and χ'' associated with the individual spin packets of the inhomogeneously broadened line are given by

$$\chi'=\frac{M_0\gamma(\omega_0-\omega)}{2\{(\omega_0-\omega)^2+\gamma^2[H_2^2+2(\delta H)^2]\}}, \tag{16}$$

$$\chi''=\frac{\gamma^2[H_2^2+2(\delta H)^2]H_0M_0}{2\{(\omega-\omega_0)^2+\gamma^2[H_2^2+2(\delta H)^2]\}T_1H_2^2\omega}, \tag{17}$$

where

$$(\delta H)^2=\tfrac{1}{3}\langle(\Delta H)^2\rangle_{\rm av}+\frac{I(I+1)}{\hbar^2\gamma^2N}\sum_{k>j}\tilde{A}_{jk}^2. \tag{18}$$

Here $\langle(\Delta H)^2\rangle_{\rm av}$ is the second moment of the unsaturated resonance line, while the second term is a sum over the number of spins N of a contribution to the linewidth from $\tilde{A}_{jk}\mathbf{I}_j\cdot\mathbf{I}_k$, the indirect spin interaction between like nuclear spins. This term at low rf levels, $\gamma^2H_2^2T_1T_2\ll1$, narrows the resonance line, while at higher rf levels, $\gamma^2H_2^2T_1T_2\gg1$, it broadens the line. We will see in Sec. IV(C) that, in the enriched nickel, where the indirect spin exchange is strong, and at low temperature, where $\gamma^2H_2^2T_1T_2\gg1$, it is a broadening mechanism. The total width of the inhomogeneous line then broadens according to

$$1/T_2^{*\prime}=(1/T_2^*)+\gamma[H_2^2+2(\delta H)^2]^{1/2}, \tag{19}$$

with δH given by Eq. (18).

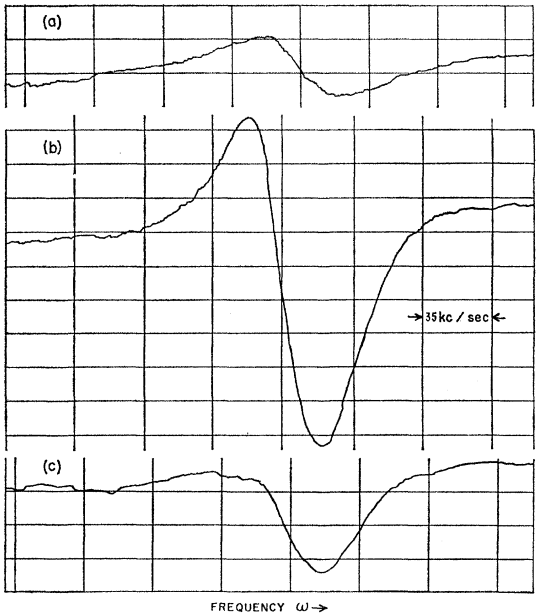

FIG. 3. (a) First derivative of observed resonance curve for sample annealed at 500°C at a low applied rf level. (b) First derivative of the resonance curve at the same applied rf level for sample annealed at 1100°C. (c) First derivative of the resonance curve for the sample annealed at 1100°C at a high applied rf level.

IV. EXPERIMENTAL OBSERVATIONS AND RESULTS

A. Line Shape Studies of Unenriched and Enriched Nickel at Room Temperature

We have studied the Ni^{61} resonance at room temperature in a number of initially strained, unenriched Ni powders with different annealing temperatures as a function of rf level. The first derivative of the Ni^{61} resonance from pure (99.99%) nickel powder annealed at 500°C is shown in Fig. 3(a). The line shape fits reasonably well the first derivative of a Lorentz absorption. The rf level used was 0.4 V (peak) across the coil. In Fig. 3(b) the resonance at the same rf level from a sample annealed at 1100°C for 1 h is shown. This line has more dispersion character and can be fitted to a Lorentz shape if one assumes β to be about 0.75. In addition, there seems to be some asymmetry, such that the resonance line extends further out on the higher frequency side. Figure 3(c) is the same as Fig. 3(b) except that the rf level is about five times as high. This line is a nearly perfect Lorentz dispersion, with some

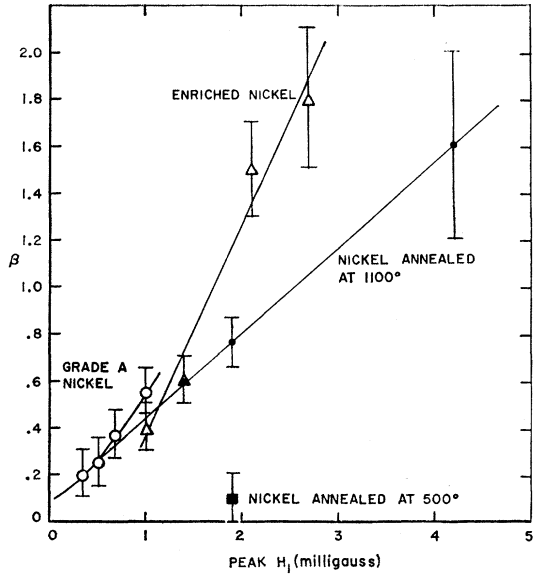

FIG. 4. Dependence of the mode-mixing parameter β on the applied rf field.

asymmetry. A similar asymmetry appears in the resonance from pure cobalt metal.[18]

The experimental curves may be fitted to Lorentz line shapes, obtaining a corrected linewidth, as well as the parameter β. Table II summarizes the results for the unenriched nickel samples annealed at 500 and at 1100°C.

TABLE II. Deduced mode mixing parameter β and linewidths at room temperature, as a function of rf level and state of anneal, for unenriched nickel.

H_1 (mG)	β	$\Delta\nu$ (kc/sec)	Anneal temp (°C)
1.9	0.1 ±0.1	60±10	500
1.4	0.6 ±0.1	45±10	1100
1.9	0.75±0.1	36±10	1100
4.2	1.6 ±0.4	39±10	1100
9.4		75±15	1100

The parameter β is plotted as a function of rf field for the sample annealed at 1100° and the sample annealed at 500° in Fig. 4. The rf field is calculated from the coil geometry and the rf voltage. We have also observed the resonance from unannealed Grade A pure carbonyl nickel which was relatively unstrained as received. From the line shape and signal intensity, this would correspond to the strained nickel annealed at about 800°. The comparison with signal intensity is made using the plot of peak-to-peak signal intensity as a function of temperature of anneal given in Fig. 5. The Grade A nickel was available in a larger quantity than the other samples and, by using a larger rf coil, a lower H_1 could be obtained with the same rf voltage. In Fig. 4 we also plot β for this nickel. For this sample it appears that the value of β in the limit of low rf level, β_0, is about 0.1.

Reference to Fig. 4 shows that in all of these nickel samples the amount of dispersion increases with rf level. This increase can be understood in terms of the theory of Sec. III based on the Bloch equations since $T_1=T_2$ in the unenriched nickel.

We also see that for the same rf level if one compares the β's for the various samples, then within experimental errors, the nickel annealed at higher temperatures has more dispersion than the poorly annealed nickel. Part of this may be due to the fact that the well-annealed nickel has a larger enhancement due to a larger initial permeability, but also β_0 is expected to be less in the poorly annealed sample as a result of less eddy current losses, as discussed in Sec. III. Since in Sec. III we estimated a μ about twice as large in the sample annealed at 1100° as in the sample annealed at 500°, we might expect a correspondingly larger value of the eddy current losses and β_0 in the sample annealed at 1100°. If the mode-mixing parameter β_0 of 0.02 estimated in Sec. III is appropriate to a sample annealed at say 500°, then the well-annealed samples might be expected to have β_0's two or three times as large, due to the larger initial permeability, in approximate agreement with the β_0 observed.

We can use the value of β_0 of 0.1 observed for the Grade A nickel sample to estimate the enhancement of the rf level in this sample. From Eq. (14) we have $\beta=\beta_0(1+\gamma^2H_2^2T_1T_2)^{1/2}$. Let $H_2=\eta H_1$ where η is the rf enhancement. Since $T_1=T_2=0.35\times10^{-3}$ sec, $\gamma=2.2\times10^3$ G^{-1} sec[19] and β will be about 1 when $H_1=2.0\times10^{-3}$ G (see Fig. 4), we obtain an η of about 7×10^3.

For the nickel annealed at 1100°, we have also measured the relative signal intensities of the absorption and dispersion modes as a function of rf level. The results are shown in Fig. 6. The intensity measurements are only approximate because of the rapid decrease in sensitivity of the circuit at higher rf levels, which had to be corrected for. The behavior of the individual absorption and dispersion modes are in approximate agreement with that given by Eq. (12).

Table II shows that there is broadening with rf level at the higher rf levels. The origin of this broadening can be seen by rewriting Eq. (7) in the form [using Eq. (14)]

$$\Delta\nu=\frac{1}{\pi T_2^{*\prime}}=\frac{1}{\pi T_2^{*}}+\frac{1}{\pi T_2}\left(\frac{\beta}{\beta_0}\right). \tag{20}$$

Taking $\beta_0=0.1$, $T_2=0.35\times10^{-3}$ sec, and $1/\pi T_2^*$ about 45×10^3 cps

$$\Delta\nu\simeq45\times10^3+10\times10^3\beta \text{ cps},$$

which explains the broadening at the higher rf levels.

There also appears to be some narrowing of the resonance line at intermediate rf levels. This narrowing

[18] Ref. 1, p. 20.

[19] R. L. Streever, Jr., Phys. Rev. Letters **10**, 232 (1963).

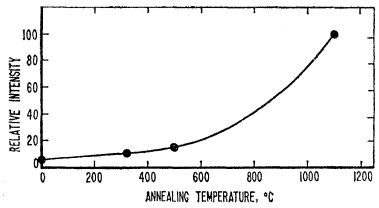

FIG. 5. Signal intensity in pure unenriched nickel as a function of annealing temperature.

of the line is probably related to that discussed by Redfield. In Fig. 6 of this paper[6] he shows the dispersion derivative at resonance as a function of $\gamma^2H_2^2T_1T_2$ both for the case of pure dipolar coupling and also for the case of strong exchange-type coupling. The narrowing in the unenriched nickel is probably related to the first case, while for the enriched nickel to be discussed next, the second case is more appropriate.

The broadening in the nickel annealed at 500° is probably a real inhomogeneous broadening and due to strains. A similar broadening with strain has been observed in the case of the Fe^{57} resonance in pure iron.[20]

We have also studied the resonance from enriched Ni^{61} as a function of rf level. The results are given in Table III and Fig. 4.

TABLE III. Deduced mode-mixing parameter β and linewidths at room temperature, as a function of rf level for enriched nickel.

H_1 (mG)	β	$\Delta\nu$ (kc/sec) (±8)
1.03	0.4±0.1	56
1.37	0.6±0.1	86
2.09	1.5±0.2	98
2.73	1.8±0.3	104

The enriched nickel was of about the same particle size as the unenriched. The enriched nickel was annealed only at about 300° so that a somewhat smaller value of β_0 is expected, as is indicated in Fig. 4. From Fig. 4 we also see that β increases more rapidly than for the unenriched nickel. We can understand this qualitatively as a consequence of the fact that $T_2<T_1$ ($T_2=0.15$ msec, $T_1=0.35$ msec) for the enriched nickel.[16] The simple theory of saturation based on the Bloch equations no longer holds and the Redfield theory should be used. We have not, however, extended Redfield's results to the case of inhomogeneously broadened lines, but instead apply his theory in a qualitative way to this case.

The greater linewidth in the enriched nickel is interesting since one is at first tempted to attribute this to a few tenths of a percent of impurities. The broadening can be seen by comparing Tables II and III. Even at the low rf levels the enriched nickel is broader than the unenriched nickel, and this may be due to the impurities or to the fact that the enriched nickel was only annealed at about 300°. The greater additional broadening in the enriched nickel at the higher rf levels, however, is probably due to the exchange-type broadening between like nuclei which comes in for $\gamma^2H_2^2T_1T_2>1$ and is given by Eq. (18). At $H_1=1\times10^{-3}$ G from Fig. 4, we see that $\gamma^2H_2^2T_1T_2>1$, so that Eq. (18) is valid. From Eqs. (18) and (19) the additional width over that from the inhomogeneous broadening is (in G)

$$\left[H_2^2+\tfrac{2}{3}\langle(\Delta H)^2\rangle_{\rm av}+\frac{2I(I+1)}{\hbar^2\gamma^2N}\sum_{k>i}\tilde{A}_{jk}^2\right]^{1/2}. \quad (21)$$

With $T_1=0.35$ msec, $T_2=0.15$ msec, and $\gamma^2H_2^2T_1T_2>1$, the second term is small compared to the first term. At the same rf level, the difference in enriched and unenriched nickel linewidth can be attributed to the third term. We defer the discussion of this to Sec. IV(C) where the above equation is more nearly applicable due to larger values of $\gamma^2H_2^2T_1T_2$, and where the difference in widths was greatest. That H_2 itself is not broadening the line appreciably at room temperature at say an H_1 of approximately 1×10^{-3} G or an H_2 of approximately 5 G, can be seen from the fact that the inhomogeneous width is about 100 G.

IV(B). External Magnetic Field Effects

We have studied the effect of an external applied magnetic field on the nuclear resonance signal from the enriched nickel.[21,22] A plot of the amplitude of resonance signal as a function of the magnetic field is shown in

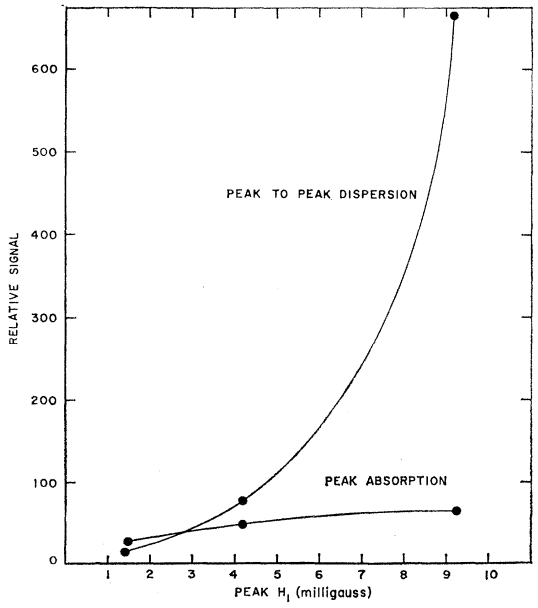

FIG. 6. The relative signal intensities for the absorption and dispersion modes plotted against the applied field H_1 for the unenriched nickel sample annealed at 1100°C.

[20] S. Ogawa and S. Morimoto, J. Phys. Soc. Japan **16**, 2065 (1961).

[21] A brief account was presented earlier by R. L. Streever and L. H. Bennett, Bull. Am. Phys. Soc. **5**, 491 (1960). Some of the temperature data was shown in L. H. Bennett and R. L. Streever, J. Appl. Phys. **33**, 1093 (1962).

[22] J. I. Budnick, Bull. Am. Phys. Soc. **7**, 295 (1962).

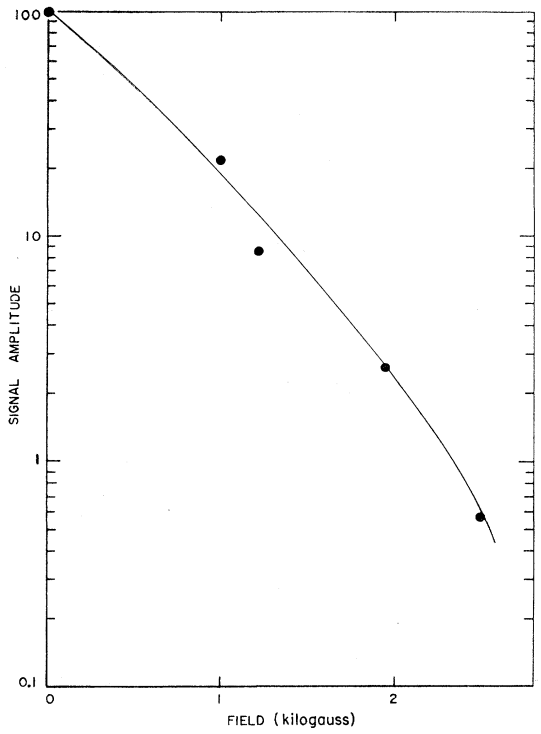

FIG. 7. Semilogarithmic plot of the relative signal amplitude as a function of externally applied dc magnetic field.

Fig. 7. A geometry was used in which the rf coil was at right angles to the dc magnetic field. In fields of 1000 G or less, the first effect seems to be a reduction in the enhancement of the rf level which leads to a reduced signal and a change in line shape (similar to that observed by decreasing the applied rf level). In higher fields the number of domain walls decreases as well, and the signal drops quickly. At about 2500 G there appeared to be some tailing of the resonance to lower frequency. The greatly reduced signal at this field, however, made measurement of a frequency shift difficult. One expects a shift of the resonance to lower frequency at about this field since the signal at fields of this size or larger are due to nuclei in the domains. For these nuclei, the resonant frequency decreases in an external applied field since the hyperfine field is negative.

IV(C). Effects of Temperature

The resonance of both the enriched nickel and unenriched nickel has been studied[21] at 300, 197, 77, and 4.2°K. The rf level used was low, an H_1 of about 1×10^{-3} G, so that the direct contribution of H_2 ($\sim$5 G) to the linewidth should be small. The line shape at low temperatures, at the same rf level, became more nearly a dispersion shape, as expected from the change in the saturation parameter. For convenience, a table of T_1 and T_2 data from the paper[16] of Weger, Hahn, and Portis is included in Table IV. At 201 and 77°K there is still some absorption present, while at 4.2°K a more nearly pure dispersion is observed. The signal is complicated at the lower temperatures by fast modulation effects.[23] The dispersion signal reaches a maximum at some phase of the lock-in detector shifted from the lock-in detector phasing at room temperature. At 4.2 and 77°K, the dispersion mode first derivative line shape has the shape of the first derivative of the Lorentz dispersion, with a slight asymmetry causing the tail to be greater on the high-frequency side of the line. Although we have not made a systematic analysis of the fast modulation effects, they are evidently a consequence of the large values of $\omega_m T_1$, where ω_m was the modulation frequency 40 cps. The signal at 4.2°K appeared to be shifted about 90°, indicating $\omega_m T_1 > 1$, with a somewhat smaller shift at 77°K. In the enriched nickel the absorption mode had a width of 360 kc/sec, somewhat less than the dispersion width. The linewidth and temperature data[21,24,25] are summarized in Table V for the enriched as well as the unenriched nickel samples. At 77 and 4°K the dispersion widths are given.

TABLE IV. Relaxation time data for enriched and unenriched nickel from Weger, Hahn, and Portis.[a]

Temperature (°K)	Enriched and unenriched T_1 (msec)	Unenriched T_2 (msec)	Enriched T_2 (msec)
295	0.35	0.35	0.15
77	1.5–2.5	1.5–2.5	0.23
4.2	15–25	8	···

[a] See Ref. 16.

TABLE V. Linewidths and resonance frequencies for the enriched and unenriched nickel.

T (°K)	ν (Mc/sec)	$\Delta\nu$ (kc/sec)
	(a) Unenriched nickel	
4.2±0.1	28.46 ±0.03	480±100
77.0±0.1	28.26 ±0.02	150±60
201.0±0.4	27.34 ±0.02	70±30
274.6±0.1	26.483±0.02	80±30
297.8±0.2	26.127±0.01	45±10
	(b) Enriched nickel	
4.2±0.1	28.47 ±0.03	580±80
77.0±0.1	28.28 ±0.03	500±100
201.4±0.4	27.37 ±0.03	100±30
274.3±0.1	26.493±0.02	90±30
297.1±0.2	26.144±0.01	56±10

The frequency has been determined by picking, as the center of the line, a point the appropriate distance between the larger peak (A of Fig. 2) and the crossover point, this distance being determined by the amount of dispersion present. In picking the center this way, one neglects the asymmetry in the line which is such as to shift the center to higher frequencies. We have neglected this asymmetry since it is about equal to or less than

[23] K. Halbach, Helv. Phys. Acta, **27**, 259 (1954).
[24] T. Hihara, T. Kushida, Y. Koi, and A. Tsujimura, J. Phys. Soc. Japan (to be published).
[25] J. I. Budnick, Bull. Am. Phys. Soc. **5**, 491 (1960).

quoted errors, and since with the method used neglecting the asymmetry is more consistent. The asymmetry seems to be greater when $\gamma^2 H_2^2 T_1 T_2 > 1$ and may be due to nickel nuclei further from the center of domain walls, which have smaller values of H_2. Thus, the values of ν quoted may be more appropriate to nuclei near the wall centers.

The difference in frequency between the enriched and unenriched nickel can be measured more accurately than the centers of the line itself, and the difference in frequency between the enriched and unenriched nickel is given in Table VI and appears to be significant. The

TABLE VI. Difference between enriched and unenriched nickel frequencies.

T (°K)	ν (enriched) $-\nu$ (unenriched) (kc/sec)
4.2	+10
77	+20
201	+30
274	+6
297	+6

difference in frequency between the enriched and unenriched nickel is always such that the enriched nickel frequency is greater. The maximum difference in frequency seems to occur around 200°K. A somewhat similar behavior was noted[26] for the case of Fe^{57} resonance in pure iron. The enriched Fe^{57} sample was found to be 15 kc/sec higher in frequency at room temperature than the unenriched sample. They explained their results as an isotope effect due to the mass difference. Kogan and Bulatov[27] have measured the dependence of the isotop e effect on the lattice parameter for Ni^{58} and Ni^{64}. Using their result, together with the volume dependence of the resonance frequency in nickel,[24] one can estimate that the enriched-nickel frequency at 77° should be about 9 kc/sec higher than the unenriched-nickel frequency from this effect alone.

Another possibility is that the isotope frequency shift is due to the longitudinal terms in the indirect exchange interaction. The transverse terms lead to the excess broadening discussed earlier in this paper. The maxima in the excess broadening and in the frequency shift occur for nickel at about the same temperature.

Since the direct contribution of the unsaturated width can be seen from the values of T_2 to be small compared to the inhomogeneous width, we believe the linewidths in the unenriched nickel are approximately inhomogeneous widths, while the additional broadening in the enriched nickel is due to the indirect coupled interaction discussed previously. The rapid increase in the linewidth in the enriched nickel between room temperature and 77° probably represents the dotted region of curve (b) of Fig. 6 of Redfield's paper.[6] That the larger width in the enriched nickel at 77°K is a high rf level effect has been verified by an independent experiment. The free precession echo was observed[28] and the echo width was found to be approximately the same for both the enriched and the unenriched nickel. Assuming a Lorentz line shape, this echo width corresponds to a linewidth approximately equal to that measured by the cw technique for the unenriched nickel. The near equality of the widths in the enriched and unenriched samples at 4.2°K indicates that the inhomogeneous broadening has taken over.

Suhl and Nakamura[29,30] have proposed a mechanism which couples nuclei in a ferromagnet through virtual excitation of spin waves. For 100% enriched nickel, using appropriate values for the anisotropy and exchange constants, this mechanism leads to a contribution to the Van Vleck second moment $(\langle \Delta\nu^2 \rangle_{\mathrm{av}})^{1/2}$ of about 200 cps. Winter[11] has shown that this mechanism should be larger for nuclei in the domain walls by a factor which is about 20 in nickel at 77°K. In a ferromagnet at temperatures well below the Curie point the Suhl interaction is highly anisotropic and would contribute to T_2. The exact calculation of T_2 from this interaction is difficult because one doesn't know in detail how the line is inhomogeneously broadened. In any case, this mechanism seems too small to be the cause of the line broadening we observe.

Another mechanism which has been used to explain saturation effects in the nonferromagnetic metals is the Ruderman-Kittel interaction[31] in which the nuclei are coupled by conduction electrons. The mechanism has the form of the last term in Eq. (21). In copper, Redfield could explain his high rf level results by taking $(\delta H)^2 = 10$ G or $\Delta\nu$ about 4 kc/sec for Cu^{63}. For 100% isotopic abundance this would be a 5 kc/sec contribution to the linewidth. In a ferromagnetic material one expects the coupling of the nuclei with the conduction electrons to be larger due to the (*sd*) interaction[32], and T_1 is a measure of this coupling. From the theory of the indirect exchange interaction and the Korringa theory we might expect that since T_1T in nickel is about an order of magnitude shorter than T_1T in copper, that the indirect coupling constant A_{jk} would be about ten times larger in nickel than in copper, giving about a 50-kc/sec contribution to $\Delta\nu$ in the enriched nickel. If the Ruderman-Kittel mechanism were enhanced this way it would seem to be a more important source of line broadening in our case.

Another effect which is related to the Suhl indirect coupling is the frequency pulling phenomena described by deGennes *et al.*[33] This effect predicts a shift in the

[26] C. Robert and J. M. Winter, Compt. Rend. **250**, 3831 (1960).
[27] V. S. Kogan and A. S. Bulatov, Zh. Eksperim. i Teor. Fiz. **42**, 1499 (1962) [translation: Soviet Phys.—JETP **15**, 1041 (1962)].
[28] R. L. Streever, Bull. Am. Phys. Soc. **7**, 614 (1962).
[29] H. Suhl, J. Phys. Radium **20**, 333 (1959).
[30] T. Nakamura, Progr. Theoret. Phys. (Kyoto) **20**, 542 (1958).
[31] M. A. Ruderman and C. Kittel, Phys. Rev. **96**, 99 (1954).
[32] M. Weger, Phys. Rev. **128**, 1505 (1962).
[33] P. G. deGennes, P. A. Pincus, F. Hartmann-Boutron, and J. M. Winter, Phys. Rev. **129**, 1105 (1963).

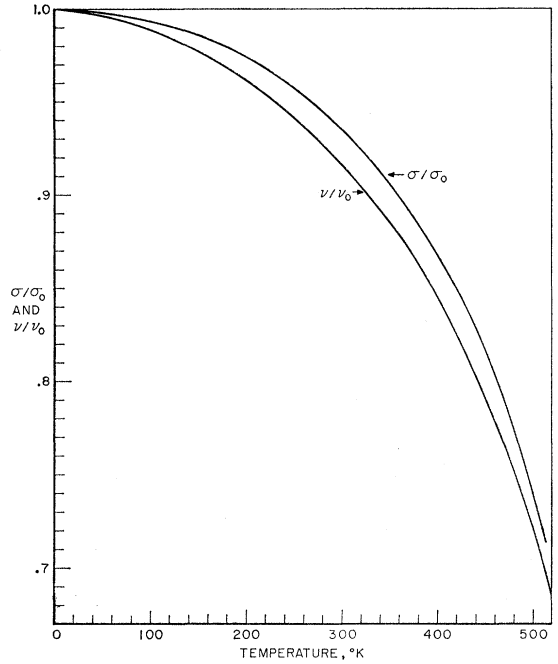

FIG. 8. A plot of reduced resonance frequency ν/ν_0 and reduced spontaneous magnetization σ/σ_0 (at constant pressure) against temperature.

resonance frequency ω_0 by an amount

$$\omega=\omega_0[1-\tfrac{1}{2}\eta_{\max}(m_0/M_0)]. \quad (22)$$

Here $\eta_{\max}$ is the maximum rf enhancement, m_0 is the macroscopic nuclear magnetic moment, and M_0 the macroscopic electronic moment. From this equation with $\eta=7\times10^3$ we obtain for enriched nickel $\Delta\nu$ about 0.5 kc/sec at 77°K or 10 kc/sec at 4°K. Since η varies as one goes along the domain wall, this would show up as a line broadening as well as a shift. This mechanism would become more important to the width at lower temperatures than used in this paper.

The super-regenerative circuit was used to observe the nuclear resonance above room temperature. The results are shown in Table VII.

TABLE VII. Nuclear resonance frequency above room temperature, using the super-regenerative circuit.

T (°K)	ν (Mc/sec)
302±1	26.04±0.1
364	24.93
431	23.11
472	21.72
489	21.07
498	20.63
517	19.64
529	18.98
536	18.58

The resonance frequency ν will be related to the spontaneous magnetization σ through the relation $\nu=A\sigma$. A will, in general, depend on temperature, both explicitly and also implicitly through the change in atomic volume with temperature.[34] The ratios ν/ν_0 and σ/σ_0 are plotted in Fig. 8 as a function of temperature. ν_0 and σ_0 are the values of ν and σ at 0°K. For the spontaneous magnetization we have used values of Foner [35] (extrapolated to $H=0$) up to 292°K and data of Weiss and Forrer[36] from 292 to 520°K. One sees from Fig. 8 that at constant pressure the temperature dependencies of ν and σ are not the same. Both the resonance frequency and the spontaneous magnetization can be computed at constant volume using the value for[24] $(1/\nu)d\nu/dp$ and the value of[37] $(1/\sigma)d\sigma/dp$ together with the compressibility[38] and the thermal expansion data.[39] At constant volume σ/σ_0 and ν/ν_0 are found to agree over the temperature range 0 to 450°K to better than 0.5%. Whether the remaining difference indicates an implicit dependence of A on temperature or is a result of inaccuracies in σ or in correcting for the volume effects is uncertain. Pugh and Argyle[40] have also measured σ from 4.2 to 120°K. Their measurements go up only to 120°K and were not shown in Fig. 8. When compared with the nuclear resonance data (at constant volume) their data agree within our experimental error with the nuclear resonance data.

V. CONCLUSION

The nuclear resonance absorption line of nickel consists of a mixture of χ'' and χ', of Lorentz shape, with some asymmetry. The effective rf level at the nucleus is about 7000 times the applied rf level for well-annealed nickel. At low applied rf levels the ratio of dispersion to absorption present is about $\beta_0=0.1$. With increasing rf, this ratio increases due to saturation effects to give a nearly perfect dispersion signal.

In the enriched nickel indirect interaction between the nuclear spins broadens the resonance line at low temperatures and high rf levels. The frequency in the enriched nickel, in addition, appears to be shifted to higher frequency compared to the unenriched nickel.

The temperature dependence of the resonance frequency and the spontaneous magnetization of the nickel agree more closely when both are corrected to constant volume.

ACKNOWLEDGMENTS

We would like to thank V. M. Johnson, D. E. Brown, G. A. Uriano, and R. D. Robbins for technical assistance.

[34] G. B. Benedek and J. Armstrong, Suppl. J. Appl. Phys. **32**, 106 (1961).
[35] S. Foner and E. D. Thompson, Suppl. J. Appl. Phys. **30**, 229 (1959).
[36] P. Weiss and R. Forrer, Ann. Phys. (Paris) **5**, 153 (1926).
[37] E. I. Kondorskii and V. I. Sedov, Zh. Eksperim. i Teor. Fiz. **38**, 773 (1960) [translation: Soviet Phys.—JETP **11**, 561 (1960)].
[38] P. W. Bridgman, *Physics of High Pressures* (G. Bell and Sons, London, 1949).
[39] F. Nix and D. Mac Nair, Phys. Rev. **60**, 597 (1941).
[40] E. W. Pugh and B. F. Argyle, J. Appl. Phys. **33**, 1178 (1962).